Apparent Size-Dependent Growth of Potash Alum Crystals by Agglomeration

Masaaki Yokota and Noriaki Kubota
Dept. of Applied Chemistry and Molecular Science, Iwate University, Morioka 020, Japan

Crystal growth rate in multiparticle systems, which is a kinetic parameter required for the design of industrial crystallizers and their operation, is evaluated by analysis of size distributions of crystals produced from Mixed Suspension Mixed Product Removal (MSMPR) crystallizers (Randolph and Larson, 1988). We often, however, encounter a crystal-size distribution (CSD) which exhibits a nonlinear curve in the population density plot (semilogarithmic population density vs. crystal-size plot). In such a case, it is difficult to deduce the growth rate using the population balance concept. The nonlinearity has been explained by assuming a size-dependent growth rate (Garside and Jancic, 1976; Mydlarz and Jones, 1990). However, the mechanism of the size-dependent growth has not been clarified yet.

Garside and Jancic (1976) measured transient CSDs of K-alum small crystals (3 to 70 μm) in a small stirred vessel. They explained the transient CSDs in terms of a size-dependent growth rate. On the other hand, Kubota and Mullin (1984) pointed out the occurrence of an agglomeration of K-alum crystals (5 to 100 μm) by showing a decrease in the number of crystals with experimental time similar to those of Garside and Jancic (1976). However, they did not show any other experimental and theoretical evidence.

This article shows the importance of agglomeration from a theoretical analysis of transient CSDs in terms of population balance with agglomeration and photomicrographic observation of suspended crystals, and then explains the apparent size-dependent growth rate by an agglomeration mechanism.

Experimental Studies

CSD measurements in a small agitation vessel

The experimental setup and procedure were similar to that of Garside and Jancic (1976). A crystallizer (550 mL) is a glass agitation vessel fitted with a jacket. A sampling probe of an electro zone sensing particle counter (ELZONE 180XY) was inserted directly into the vessel, and the size distribution of crystals (Berglund, 1992) were measured. We selected a sampling probe with a relatively large-size orifice (240 μm in dia.) to avoid blocking caused by the crystals to be measured. The measured size range was 5 to 100 μm.

A solution at a given saturation temperature was prepared by dissolving a prescribed amount of K-alum crystals in water in the vessel. After the solution was cooled to a fixed operational temperature (30.0°C), small crystals (secondary nuclei) were generated by contacting a K-alum parent crystal, glued to the top of a stainless wire with the impeller. After a contact, the parent crystal was removed immediately from the solution and only the newly formed crystals were grown in the suspension (400 rpm). During growth, the suspensions were sampled through an orifice of the probe at 5 min intervals, and CSDs were measured. Growth rates G_{SUS} nucleation rates B_o and agglomeration rate constants k_a were evaluated by fitting a population balance equation (Eq. 1, see below) with the measured CSDs.

After finishing a run, the slurry was sampled and kept stationary in a glass vessel. The sampled crystals were observed under an optical microscope at room temperature.

Growth rate measurements of fixed small crystals

For comparison, growth rates of fixed small crystals, which are free from crystal-crystal interactions, were measured in a flow cell. The solution, stored in a thermostatically controlled tank (30°C), was passed to the flow cell, which was set on the stage of an optical microscope. The flow was stopped for a while. Some small crystals appeared on the bottom of the cell. After they grew to the desired size (25 to 100 μm), the solution was continuously fed into the cell. Some of the small crystals were removed from the cell, while some others remained and their size was measured with time. The growth rates of the fixed small crystals G_{fix}, were determined from the slope of size vs. time plots.

Results and Discussion

Variations of CSDs

Typical examples of measured size distributions of small crystals are shown in Figures 1a to 1d on a cumulative oversize number basis. In lower supersaturations (Figures 1a and 2b), ($t >$ 5 min) transient behavior of CSDs similar to those

---

Correspondence concerning this work should be addressed to M. Yokota.

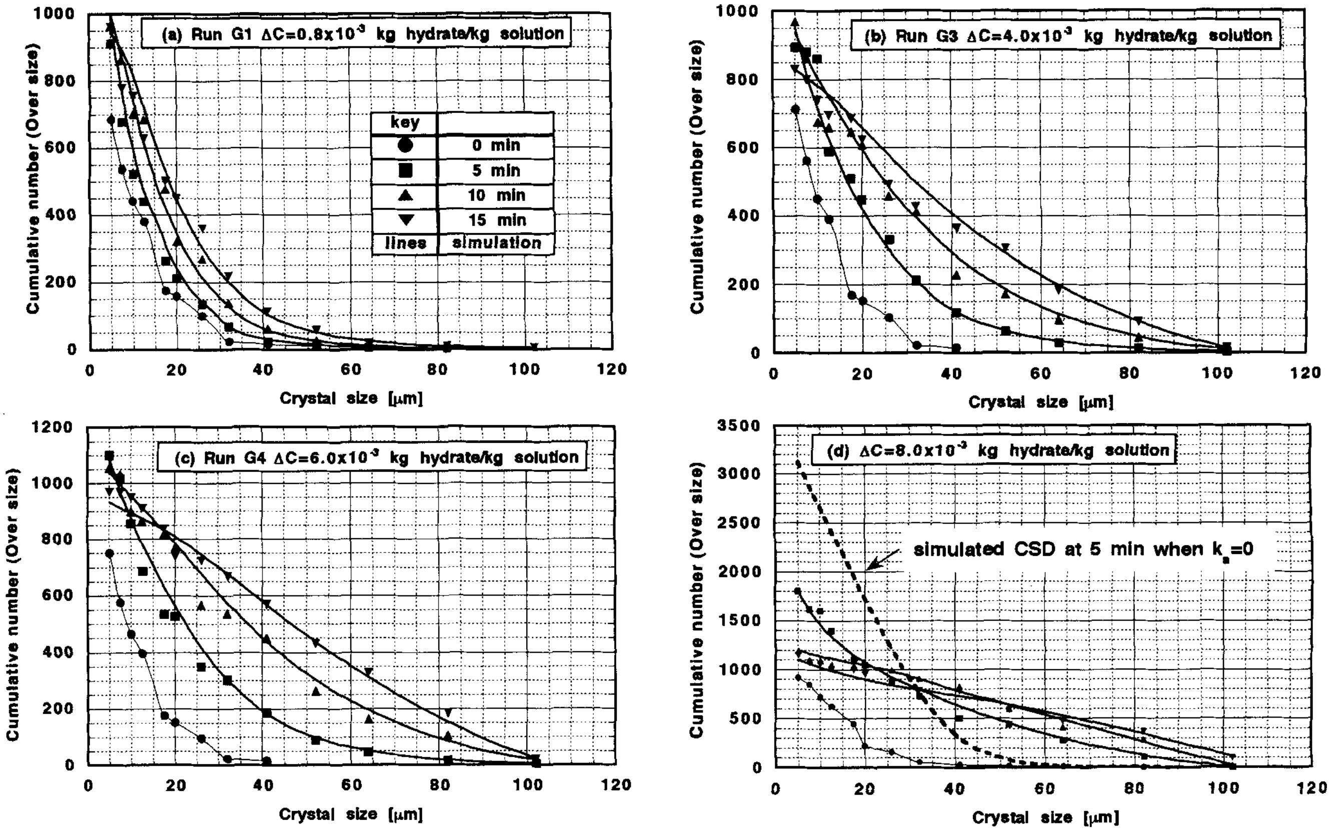

Figure 1. Simulated and measured CSDs at different supersaturations.

Operational temperature = 30.0°C; impeller speed = 400 rpm.

of Garside and Jancic (1976) can be seen. On higher supersaturations (Figures 1c and 1d), however, the total number of crystals larger than 5 μm (N_{L1}) decreased especially after 5 min. These types of transient CSDs are similar to Kubota and Mullin (1984). Microscopic observation of the crystals sampled at the end of run showed the existence of agglomerated crystals even in case of the lowest supersaturation (Figure 1a). Their population increased with supersaturation. Therefore, we must take into account the effect of agglomeration in analyzing the transient CSD in multiparticle systems.

We try to explain the transient CSDs in Figure 1a to 1d in terms of a population balance with agglomeration and constant growth rate. The crystalline particles less than L_1 (lowest measurable crystal size) could not be counted in our experiments, although these particles play an important role in the development of CSD (we call these particles nuclei for convenience). This is a serious problem in CSD development modeling. The nuclei behave in the same way as crystals larger than L_1 (called crystal), i.e., nuclei grow and agglomerate. In formulating a population balance equation, we make the following assumptions: (1) The nucleation rate (effective) is the number of nuclei remaining the size range larger than L_1 due to growth or by agglomeration; (2) the remaining nuclei adhere to the larger crystals. These larger crystals grow by this type of agglomeration (agglomeration growth mechanism), as well as by the ordinary molecular level growth mechanisms; (3) the combined growth rate is assumed to be size-independent; (4) the larger crystals are assumed to agglomerate by collisions between two crystals. On the basis of these assumptions, a population balance equation (Eq. 1) is formulated

$$\frac{\partial f(L,t)}{\partial t} + G_{\text{sus}}\frac{\partial f(L,t)}{\partial L} = B_o \cdot \delta(L - L_1) + \frac{k_a}{2}\int_{L_1}^{L} f(L-x)\cdot f(x)dx - k_a\int_{L_1}^{\infty} f(L)\cdot f(x)dx \quad (1)$$

where $f(L,t)$ is the population density, L is the crystal size, B_o is the nucleation rate, and k_a is the agglomeration rate constant. When agglomeration is occurring, volume (or mass) is taken as the internal coordinate (Glatz, Hoare, and Landa-Vetiz, 1986; Hartel and Randolph, 1986) because of the additive property of volume accompanied by agglomeration. However, we simply used size as the coordinate since virtually no difference was shown in preliminary calculations. It should be mentioned that G_{sus} includes contributions from both agglomeration growth and normal growth mechanisms. In order to transform Eq. 1 in terms of the discrete function $n(L_i,t)$

$$n_i = \int_{L_i}^{L_{i+1}} f(L,t)dL \quad (2)$$

each term of Eq. 1 was multiplied by dL and integrated between the boundaries of each size channel

$$\frac{\Delta n_i(t)}{\Delta t} = \frac{G_{\mathrm{sus}}}{\Delta L}[n_{i-1}(t) - n_i(t)] = B_o\cdot\delta(L - L_1) + \frac{k_a}{2}\sum_{k=1}^{i} n_{i-k}(t)\cdot n_k(t) - k_a\cdot n_i(t) N_{L1}(t) \quad (3)$$

Equation 3 was solved numerically using a trial-and-error method by assuming G_{sus}, B_o, and k_a to satisfy CSDs experimentally measured. The CSD measured at $t = 0$ was used as the initial condition. Calculation was performed by letting $\Delta L = 5$ μm ($= L_1$) and $\Delta t = 0.1$ s.

The solid lines in Figures 1a to 1d are the calculated curves. These curves agree fairly well with the measured CSDs. The broken line in Figure 1d is the calculated CSD at $t = 5$ min by assuming no agglomeration ($k_a = 0$). This curve is quite different from the actual corresponding CSD curve (solid curve for square symbols), which means that agglomeration has a great effect in the development of CSD. Agglomeration causes a decrease in the number of crystals in the smaller-size range, while in the larger-size range, it has the reverse effect on the number of crystals.

Kinetic parameters evaluated

Growth rates of suspended crystals G_{sus} are plotted against supersaturation in Figure 2 (open circles) on a logarithmic paper. G_{sus} increases with increases in supersaturation. The slope of the line was small in the lower supersaturation region, but became larger at higher supersaturation regions ($\Delta C > 4\times10^{-3}$ kg hydrate/kg solution). The growth rate of fixed crystals G_{fix} (closed circles), however, was correlated by a straight line with the same lower slope over the whole range of supersaturation as that of G_{sus}. The increased slope can be attributed to the agglomeration growth mechanism. Adhesion of small particles ($< L_1$) to the crystals ($\geq L_1$) contributed more extensively to growth as supersaturation increased. This type of agglomeration is thought to occur more easily as supersaturation increases; the agglomeration rate constant, discussed below, increased with increases in supersaturation.

Estimated agglomeration rate constants are shown in Figure 3. The constants increase with increases in supersaturation. The magnitude of the estimated constant is roughly of the same order of values reported for coagulation of drops in turbulent clouds (Saffman and Turner, 1956).

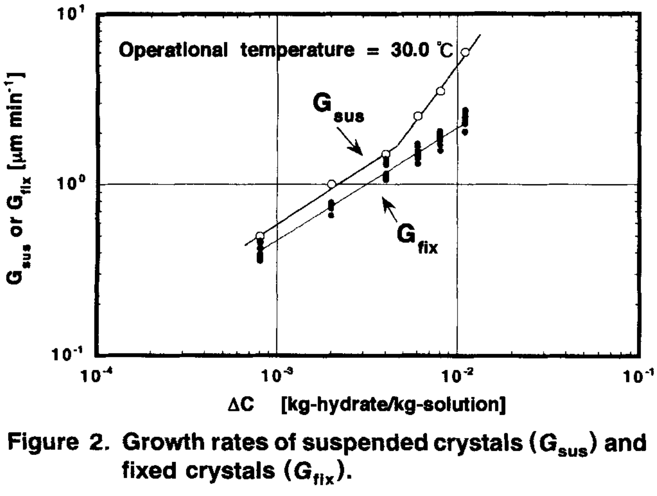

Figure 2. Growth rates of suspended crystals (G_{sus}) and fixed crystals (G_{fix}).

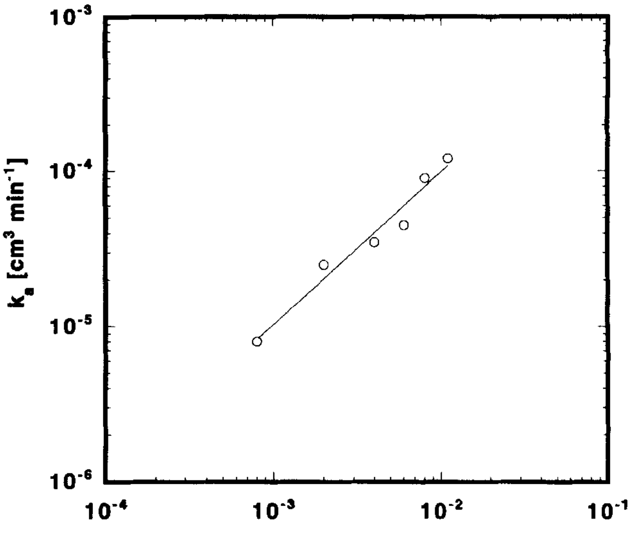

Figure 3. Corrrelation between agglomeration rate constant (k_a) and supersaturation.

The nucleation rates (B_o), defined as the birth rate of crystals of size L_1 in this article are summarized in Table 1. B_o decreased with time, which can be explained by the fact that the actual nucleation (not the generation of 5-μm-particles) occurred only at the instant of contact between the parent crystal and the impeller at the beginning of a run, with no additional production of nuclei following. B_o was supersaturation dependent. It increased with increases in the supersaturation as ordinary secondary nucleation rates, because the initial number of actual nuclei increased.

Table 1. Experimental Conditions and Nucleation Rate Evaluated*

Run No.	ΔC (kg hydrate/kg Soln.)	Time (min)	B_o ($\mathrm{cm}^{-3}\cdot\mathrm{min}^{-1}$)
G1	0.8×10^{-3}	0 ~ 5	15
		5 ~ 10	5
		10 ~ 15	1
G2	2.0×10^{-3}	0 ~ 5	20
		5 ~ 10	12
		10 ~ 15	2
G3	4.0×10^{-3}	0 ~ 5	20
		5 ~ 10	10
		10 ~ 15	3
G4	6.0×10^{-3}	0 ~ 5	26
		5 ~ 10	10
		10 ~ 15	4
G5	8.0×10^{-3}	0 ~ 5	30
		5 ~ 10	13
		10 ~ 15	4
G6	8.0×10^{-3}	0 ~ 5	41
		5 ~ 10	10
		10 ~ 15	2
G7	11.0×10^{-3}	0 ~ 5	72
		5 ~ 10	19
		10 ~ 15	6

*Operational temperature = 30.0°C.

Size enlargement caused by agglomeration (apparent size-dependent-growth)

As mentioned earlier, Garside and Jancic (1976) determined the growth rate of crystals in suspension from the displacement of the cumulative crystal-size distribution curve based on the assumption of a constant number of crystals. We achieved both Garside and Jancic (1976) and Kubota and Mullin (1984) type transient CSDs qualitatively by changing operational supersaturation. If a constant number is assumed for the CSDs for lower supersaturations (Figures 1a and 1b), then apparent growth rates can be deduced as a function of crystal size from the displacement of CSD as pointed out by Garside and Jancic (1976). Since the CSD hardly moves in the small-size range, the apparent growth rate is small. At a higher supersaturation, the apparent growth rate may become negative, since the CSD curves cross. Thus, a decrease in the number of crystals results in an apparent size-dependent growth rate.

Notation

ΔC = supersaturation, kg hydrate·(kg solution)$^{-1}$
B_0 = nucleation rate, cm^{-3}·min^{-1}
$f(L,t)$ = population density distribution function, cm^{-3}·μm^{-1}
G_{sus} = linear growth rate of suspended small crystals, mm·min^{-1}
G_{fix} = linear growth rate of fixed small crystals, mm·min^{-1}
k_a = agglomeration rate constant, cm^3·min^{-1}
L = size of crystals, μm
L_1 = lowest measurable size = 5 μm
ΔL = size interval = 5 μm
$n_i(t)$ = number of crystals in the ith channel, cm^{-3} (5 μm)$^{-1}$
N_{L1} = total number of small crystals larger than L_1, cm^{-3}
t = batch time, min
Δt = time interval = 0.1 s

Literature Cited

Berglund, K. A., *Handbook of Industrial Crystallization*, A. S. Myerson, ed., Butterworth-Heinemann, Boston, p. 89 (1992).

Garside, J., and S. J. Jancic, "Growth and Dissolution of Potash Alum Crystals in the Subsieve Size Range," *AIChE J.*, **22**, 5, 887 (1976).

Glatz, C. E., M. Hoare, and J. Landa-Vetiz, "The Formation and Growth of Protein Precipitates in a Continuous Stirred Tank," *AIChE J.*, **32**, 7, 1196 (1986).

Hartel, R. W., and A. D. Randolph, "Mechanisms and Kinetic Modeling of Calcium Oxalate Crystal Aggregation in a Urinelike Liquor, Part II Kinetic Modeling," *AIChE J.*, **32**, 7, 1176 (1986).

Kubota, N., and J. W. Mullin, "On the Decrease of Potash Alum Small Crystals Suspended in an Agitated Supersaturated Solution," *J. of Crystal Growth*, **66**, 676 (1984).

Mydlarz, J., and A. G. Jones, "On MSMPR CSD Statistics for Size-dependent Crystal Growth," *Proc. Symp. Industrial Crystallization*, A. Mersmann, ed., Garmisch-Partenkirchen, Germany, p. 417 (1990).

Randolph, A. D., and M. A. Larson, *Theory of Particulate Processes*, 2nd ed., Academic Press, New York (1988).

Saffman, P. G., and J. S. Turner, "On the Collision of Drops in Turbulent Clouds," *J. of Fluid Mechanic*, **1**, 16 (1956).

Manuscript received July 14, 1994, and revision received July 10, 1995.